

HOLLOW AND FLAT ELECTRON BEAM GENERATION AT FACET-II

A. Halavanau, C. Mayes, S. Gessner

SLAC National Accelerator Laboratory, Stanford University, Menlo Park, CA, USA

J. Rosenzweig, University of California, Los Angeles, CA, USA

Abstract

In this proceeding, we investigate hollow and flat electron beam generation at FACET-II facility. We focus on the case of a circular beamlet arrangement, also known as 'necklace' beams. We study, via numerical simulations, the resulting e-beam dynamics in the FACET-II photoinjector, beam propagation through the high energy section, as well as possible experimental applications of the 'necklace' beams. Finally, we evaluate the feasibility of high charge flat beam generation.

INTRODUCTION

Transverse shaping of electron beams is a powerful technique that can potentially enable new dielectric and plasma wakefield experiments [1–7]. In particular, highly asymmetric (flat) and hollow beams are of interest. There are several practical requirements to any transversely shaped beams in the experimental applications. First, they must survive complex accelerator beamlines, including bends, quadrupole lattices and chicanes. We note that while the corresponding beam dynamics may be addressed in simulations, typical beam dynamics codes are only well-designed to handle round, axially symmetric Gaussian beams. In case of large transverse asymmetries or voids in the e-beam phase-space, the simulation settings need to be addressed specifically to each case. Second, the transversely shaped beams must respond well to beam compression, in order to be used as wakefield "drivers" and satisfy peak current requirements. We point out that beam compression of highly asymmetric or hollow beams has not been studied in detail [8] and is yet to be understood. This makes generation and beam propagation of flat and hollow beams an important experiment by itself.

In this proceeding, we explore two methods of transverse e-beam shaping: round-to-flat beam (RTFB) transformation and micro-lens array (MLA) laser shaping. We used beam physics code *IMPACT-T* to study the FACET-II injector and *BMAD* particle tracking code to simulate e-beam propagation through the FACET-II high-energy section. In this study, we extensively utilized LUME software tools, described in Ref. [9].

NECKLACE BEAM GENERATION

Hollow beam generation in a photoinjector, with very bunch low charge, has been studied in [10]. These beams could be used as both "witness" and "driver" beams in the axially symmetric collinear wakefield accelerator (CWA) structures. Here we consider the same MLA-based spatial shaping technique to produce high energy "necklace"

beams (consisting of a ring of beamlets) with a charge of $Q = 25$ pC. For brevity we refer the reader to Ref. [11] for a detailed description of the MLA transverse laser beam shaping. A possible layout (not to scale) is shown in Fig. 1. A pulse of UV laser is propagated through the MLA shaper with a circular mask. Imaging lens system translates the segmented transverse intensity distribution onto the photocathode, producing a 12-beamlet "necklace" beam. We note that a similar MLA-based setup has been implemented at Argonne Wakefield Accelerator (AWA) and is used on a daily basis. After propagation in the photoinjector, the particle distribution is sent into the high energy linac section, and is finally delivered to the FACET-II interaction point; see Fig. 2.

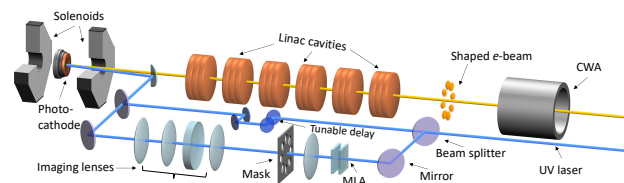


Figure 1: A schematics (not to scale) of the MLA laser shaping setup in a photoinjector facility: initial UV pulse is split into two lines, each can serve as either "witness" or "drive", with the MLA installed in one of the lines. The laser intensity in each line is controlled via beamsplitter and waveplates. Photoemitted e-beam is then shaped, accelerated and sent into a CWA (e.g. a hollow dielectric cylinder).

We note that the initial hollow structure of the e-beam is preserved, although the individual beamlets are no longer resolvable. The resulting average current is about 65 A. Further increase of the beam current is possible by increasing the charge in the photoinjector, as well as optimizing the beam transport. However, similar to their hollow donut-like counterparts [10], "necklace" beams exhibit strong sensitivity to the CSR emittance growth in the chicanes. Therefore, further theoretical, experimental, and simulation work is needed to fully establish the limits of hollow e-beam compression.

FLAT BEAM GENERATION

In order to produce flat (high transverse emittance asymmetry) electron beams, we employ a classical technique, previously studied in Refs. [12–19]. In brief, a strong magnetic field is applied at $z = 0$ m location (at the photocathode) where the electrons are generated. This results in the canonical angular momentum integral of motion and large

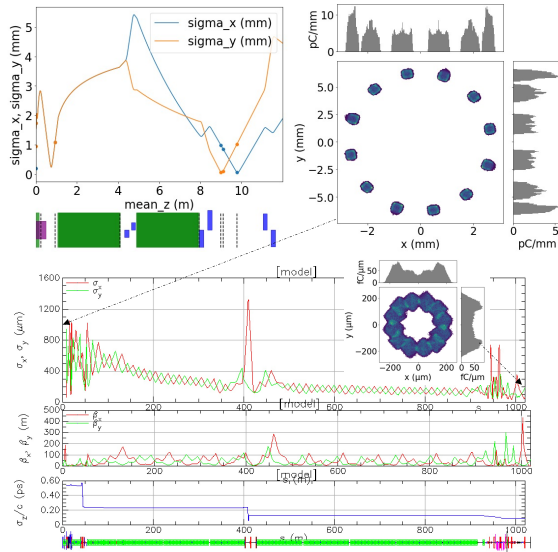


Figure 2: Start-to-end numerical simulations in IMPACT-T and BMAD of the 25 pC "necklace" beam at FACET-II. The transverse profile is maintaining the hollow structure, with a pulse duration of $\sigma_\tau = 90$ fs and average current of $I_{\text{avg}} = 65$ A.

projected x and y emittances. In addition, eigen-emittances become highly asymmetric, with one emittance being, in principle, smaller than thermal. A RTFB transformer may be employed to project the eigen-emittances onto real measured ϵ_x, ϵ_y , by diagonalizing the beam matrix.

Typically, an RTFB consists of 3 skewed quadrupole magnets. We note that 3 quadrupole solution is mathematically only valid for an axially symmetric beam. In practice, initial asymmetries stemmed from the laser hot spots result in an asymmetric beam matrix, rendering the 3 quadrupole solution to be only approximate. This was confirmed experimentally in [20] for low bunch charges and for charges up to 1 nC in [21]. With the increase of the bunch charge, the beam matrix asymmetry gets exacerbated. In our setup we add an additional quadrupole for more control over the RTFB process, in order to generate flat beams of 2 nC charge.

We also point out that there are two solutions to RTFB lattice, corresponding to horizontal and vertical flat beams. It was previously experimentally observed that horizontal flat beams are compressed with a better preservation of ϵ_{4D} [8], justifying our choice of quadrupole settings.

A field of about 0.2 T was applied at the photocathode, using the bucking solenoid, with the laser spot diameter of 5.5 mm. In order to preserve the value of CAM, we turned off all the regular quadrupoles in the injector (Fig. 3). We also set the injector acceleration cavities to -25° off-crest to compensate for the longitudinal space-charge chirp. We stated by using an analytical solution to 3 skewed quadrupole lattice, provided in Ref. [20], Eq. (6). We then used a symplectic optimizer to determine the 4 skewed quad settings to maximize the emittance ratio. We found that although

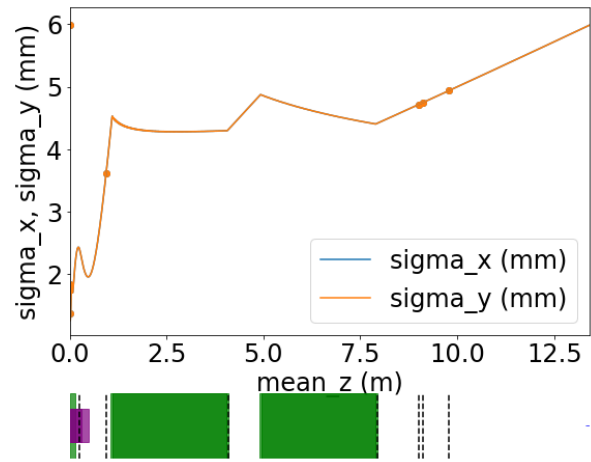


Figure 3: FACET-II injector spot-size evolution with regular quadrupoles turned off.

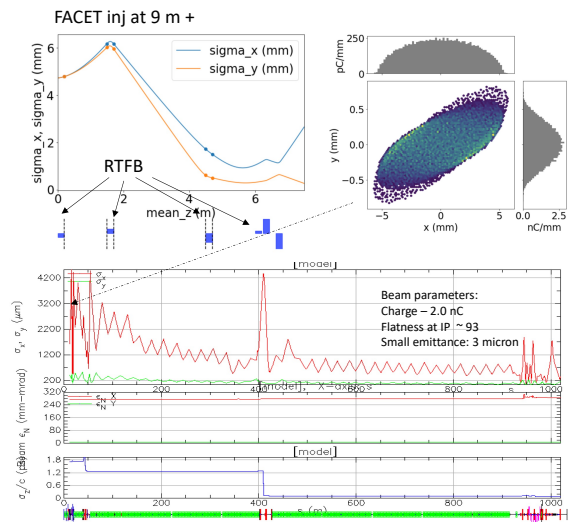


Figure 4: Start-to-end numerical simulations in IMPACT-T and BMAD of the 2 nC flat beam at FACET-II. The final attainable flatness is $\epsilon_+/\epsilon_- \approx 93$.

the 3 quadrupole solution overall gives a good initial guess. It may be used in the real machine and seed the random walk optimizer process. The final real projected emittances of 2 nC beam were $\epsilon_- = 3 \mu\text{m}$ and $\epsilon_+ = 280 \mu\text{m}$. After optimization, the beam macroparticle distribution was passed into BMAD for tracking in the high energy beamline. The results are displayed in Fig. 4. The final transverse beam size ratio needed for slab CWA experiments (e.g. dielectric slab) can be further increased (decreased) with the matching quadrupoles. We note that although we utilized the CSR model in BMAD, an in-depth study is required to quantify flat beam compression and the effects of the CSR. This topic remains largely unexplored and requires a dedicated experimental measurement program.

SUMMARY

We have demonstrated, via numerical simulations, a possibility of delivering hollow beams of 25 pC charge and flat beams of 2 nC charge to the FACET-II interaction point. We note that more work is needed to quantify the limiting factors of beam compression for both cases. Hollow and flat beams, when fully optimized, will enable new exciting CWA experiments. Given the relative simplicity of the discussed e-beam shaping techniques, we point out that some of the experimental work may as well be performed at smaller scale facilities. Finally, hollow and flat beams may serve as a beam-based accelerator diagnostics tool.

ACKNOWLEDGEMENTS

This work was supported in part by the U.S. Department of Energy Office of Science, Office of Basic Energy Sciences under Contract No. DE-AC02-76SF00515. This research used resources of the National Energy Research Scientific Computing Center, a DOE Office of Science User Facility supported by the Office of Science of the U.S. Department of Energy.

REFERENCES

- [1] N. Jain, T. M. Antonsen, and J. P. Palastro, “Positron acceleration by plasma wakefields driven by a hollow electron beam”, *Phys. Rev. Lett.*, vol. 115, p. 195 001, Nov. 2015.
doi:10.1103/PhysRevLett.115.195001
- [2] A. Tremaine, J. Rosenzweig, and P. Schoessow, “Electromagnetic wake fields and beam stability in slab-symmetric dielectric structures”, *Phys. Rev. E*, vol. 56, pp. 7204–7216, Dec. 1997.
doi:10.1103/PhysRevE.56.7204
- [3] G. Andonian *et al.*, “Dielectric wakefield acceleration of a relativistic electron beam in a slab-symmetric dielectric lined waveguide”, *Phys. Rev. Lett.*, vol. 108, p. 244 801, Jun. 2012.
doi:10.1103/PhysRevLett.108.244801
- [4] B. D. O’Shea *et al.*, “Suppression of deflecting forces in planar-symmetric dielectric wakefield accelerating structures with elliptical bunches”, *Phys. Rev. Lett.*, vol. 124, p. 104 801, Mar. 2020.
doi:10.1103/PhysRevLett.124.104801
- [5] S. Gessner *et al.*, “Demonstration of a positron beam-driven hollow channel plasma wakefield accelerator”, *Nat. Comm.*, vol. 7, no. 1, p. 11 785, 2016.
doi:10.1038/ncomms11785
- [6] S. S. Baturin and A. Zholents, “Stability condition for the drive bunch in a collinear wakefield accelerator”, *Phys. Rev. Accel. Beams*, vol. 21, p. 031 301, Mar. 2018.
doi:10.1103/PhysRevAccelBeams.21.031301
- [7] S. S. Baturin, G. Andonian, and J. B. Rosenzweig, “Analytical treatment of the wakefields driven by transversely shaped beams in a planar slow-wave structure”, *Phys. Rev. Accel. Beams*, vol. 21, p. 121 302, Dec. 2018.
doi:10.1103/PhysRevAccelBeams.21.121302
- [8] A. Halavanau *et al.*, “Bunch compression of flat beams”, in *Proc. 9th Int. Particle Accelerator Conf. (IPAC’18)*, Vancouver, Canada, Apr. 2018, pp. 3368–3371.
doi:10.18429/JACoW-IPAC2018-THPAK062

- [9] C. E. Mayes *et al.*, “Lightsource unified modeling environment (Lume), a start-to-end simulation ecosystem”, presented at the 12th Int. Particle Accelerator Conf. (IPAC’21), Campinas, Brazil, May 2021, paper THPAB217, this conference.
- [10] A. Halavanau, Y. Ding, C. E. Mayes, P. Piot, and S. Baturin, “Hollow electron beams in a photoinjector”, in *Proc. 11th Int. Particle Accelerator Conf. (IPAC’20)*, Caen, France, May 2020, pp. 49–52.
doi:10.18429/JACoW-IPAC2020-WEVIR06
- [11] A. Halavanau *et al.*, “Spatial control of photoemitted electron beams using a microlens-array transverse-shaping technique”, *Phys. Rev. Accel. Beams*, vol. 20, p. 103 404, Oct. 2017.
doi:10.1103/PhysRevAccelBeams.20.103404
- [12] Y. Derbenev, “Adapting optics for high-energy electron cooling”, Univ. Michigan, Ann Arbor, MI, USA, Rep. UM-HE-98-04-A, Feb. 1998.
- [13] P. Piot, Y.-E. Sun, and K.-J. Kim, “Photoinjector generation of a flat electron beam with transverse emittance ratio of 100”, *Phys. Rev. ST Accel. Beams*, vol. 9, p. 031 001, Mar. 2006.
doi:10.1103/PhysRevSTAB.9.031001
- [14] J. Zhu, P. Piot, D. Mihalea, and C. R. Prokop, “Formation of compressed flat electron beams with high transverse-emittance ratios”, *Phys. Rev. ST Accel. Beams*, vol. 17, p. 084 401, Aug. 2014.
doi:10.1103/PhysRevSTAB.17.084401
- [15] Y.-E. Sun *et al.*, “Generation of angular-momentum-dominated electron beams from a photoinjector”, *Phys. Rev. ST Accel. Beams*, vol. 7, p. 123 501, 2004.
doi:10.1103/PhysRevSTAB.7.123501
- [16] K.-J. Kim, “Round-to-flat transformation of angular-momentum-dominated beams”, *Phys. Rev. ST Accel. Beams*, vol. 6, p. 104 002, Oct. 2003.
doi:10.1103/PhysRevSTAB.6.104002
- [17] A. Ody, P. Musumeci, J. Maxson, D. Cesar, R. J. England, and K. P. Wootton, “Flat electron beam sources for DLA accelerators”, *Nucl. Instrum. Methods Phys. Res. A*, vol. 865, Oct. 2016.
doi:10.1016/j.nima.2016.10.041
- [18] R. Brinkmann, Y. Derbenev, and K. Flottmann, “A low emittance, flat-beam electron source for linear colliders”, *Phys. Rev. ST Accel. Beams*, vol. 4, p. 053 501, 2001.
doi:10.1103/PhysRevSTAB.4.053501
- [19] S. Nagaitsev and A. Shemyakin, “Beam emittance calculation in the presence of an axially symmetric magnetic field”, Rep. FERMLAB-TM-2107, May 2000.
doi:10.2172/754860
- [20] A. Halavanau *et al.*, “Magnetized and flat beam generation at the fermilab’s FAST facility”, in *Proc. 9th Int. Particle Accelerator Conf. (IPAC’18)*, Vancouver, Canada, Apr. 2018, pp. 3364–3367.
doi:10.18429/JACoW-IPAC2018-THPAK061
- [21] T. Xu *et al.*, “Generation high-charge of flat beams at the argonne wakefield accelerator”, in *Proc. 10th Int. Particle Accelerator Conf. (IPAC’19)*, Melbourne, Australia, May 2019, pp. 3337–3340.
doi:10.18429/JACoW-IPAC2019-WEPTS094